Water Adsorption, Dissociation and Oxidation on $SrTiO_3$ and Ferroelectric Surfaces Revealed by Ambient Pressure X-ray Photoelectron Spectroscopy

Neus Domingo,[†*] Elzbieta Pach,[†] Kumara Cordero-Edwards,[†] Virginia Pérez-Dieste,[‡] Carlos Escudero,[‡] Albert Verdaguer[§ *]

[†] Catalan Institute of Nanoscience and Nanotechnology (ICN2), CSIC and The Barcelona Institute of Science and Technology, Campus UAB, Bellaterra, 08193 Barcelona, Spain

[‡] ALBA Synchrotron Light Source, Carrer de la Llum 2−26, 08290 Cerdanyola del Vallès,Barcelona, Spain

[§]Institut de Ciència de Materials de Barcelona ICMAB-CSIC, Campus de la UAB,

E-08193 Bellaterra, Spain

*ndomingo@icn2.cat; *averdaguer@icmab.es

KEYWORDS: Ambient Pressure XPS, water, adsorption, dissociation, photocatalysis, SrTiO3, BaTiO3, BiFeO3, polarization, oxide perovskites, ferroelectricity.

ABSTRACT

In-situ natural water dissociation and redox processes on metal oxide perovskites which easily expose TiO_2 – terminated surfaces, such as $SrTiO_3$, $BaTiO_3$ or $Pb(Zr,Ti)O_3$ are studied by ambient pressure XPS, as a function of water vapour pressure. Water dissociation is of great interest because its fundamental aspects are still not well understood and it has implications in many processes, from ferroelectric polarization screening phenomena to surface catalysis and oxides surface chemistry. From the analysis of the O1s spectra, we determine the presence of different type of oxygen based species, from hydroxyl groups, either bound to $Ti^{4+}$and metal sites or lattice oxygen, to different peroxide compounds, and propose a model for the adsorbates layer

composition, valid for environmental conditions. From the XPS analysis, we describe the existing surface redox reactions for metal oxide perovskites, happening at different water vapour pressures. Among them, peroxide species resulting from surface oxidative reactions are correlated with the presence of Ti^{4+} ions, which are observed to specifically promote surface oxidation and water dissociation as compared to other metals. Finally, surface water oxidation cycle is enhanced by X-ray beam irradiation, leading to a higher coverage of peroxide species after beam overexposure.

INTRODUCTION

Surfaces under ambient conditions show a wide range of interactions with water molecules. Water can form a layer upon physical adsorption, pseudo-dissociate or chemisorb by simultaneously hydroxylating and protonating the surface or even participate in different oxidative or reducing reactions, as an oxidizing agent or in photocatalytic processes.[1] Among all surfaces, interaction with metal oxide perovskites is of great interest because its fundamental aspects are still not well understood and it has implications in many processes, from ferroelectric polarization screening phenomena to surface catalysis and oxides surface chemistry in general, as well as a strong impact in applied electronics and sensing devices. Among the studies devoted to water interaction with perovskite-type oxide surfaces, emphasis has been placed on those exposing a TiO_2 terminated surface[2-5] such as $SrTiO_3$ (STO),[6-13] $BaTiO_3$ (BTO)[14-16] or even $Pb(Zr_{0.25}Ti_{0.75})O_3$ (PZT)[17] due to its proximity with photocatalytic reactions mediated by TiO_2.[18]

Theoretical studies on water interaction with surfaces can be classified into those addressing ideal surfaces for a fundamental point of view and those which study reconstructed surfaces, closer to what can be expect for coarse materials exposed to ambient.[19-21] For STO surfaces, molecular and

dissociative adsorption has been modeled in ideal surfaces and reconstructed surfaces for both terminations (SrO and TiO_2),[7-8, 12, 14] while for BTO, several experimental and theoretical studies have been conducted to study the reactivity of water on surfaces with different configurations,[15] including their effect on ferroelectric polarization charge screening.[16, 22-25]

Furthermore, photocatalytic water splitting on different TiO_2 surfaces[14, 26] is of great interest for H_2 production[21] and in general for applications in atmospheric chemistry[27] and photocatalytic environmental cleaning.[14] Several studies of density functional theory (DFT) delve into the mechanistic picture of the nature of surface active sites for the photoinduced holes transfer from the TiO_2 surface to the adsorbed water[28] as well as the role in photocatalytic reactions[5] of water and organic compounds as intermediate products.[20, 29] It has been found that two types of hydroxyl groups (terminal hydroxyl groups, Ti-OH, and bridging hydroxyl groups, Ox-H)[28] are present on the TiO_2 surface,[2] even though their distribution and activity properties are unclear. Moreover, predicted photocatalytic reactions often include the presence of reduced ions, and several other oxide species such as surface peroxide or O_2^- adatoms that have been detected as intermediate species[28] associated to water oxidation reactions in environmental conditions. Although STO is known to perform poorly as a water oxidation site in comparison with pure TiO_2 surfaces because of the stability of the Ti(IV)-O to oxidize further,[20] in ambient pressure X-Ray photoelectron spectroscopy (AP-XPS) experiments an intense generation of material's holes can accelerate surface water catalytic reactions.

The identification of different oxygen species upon water adsorption by AP-XPS has been extensively studied for metal surfaces. On Pt[30], known to induce water dissociation, spectra taken at the O1s region revealed up to 5 different contributions from different oxygen states indicating a complex reactivity of water molecules in contact with the surface. However, the experimental

determination of water surface adsorption on oxide perovskites from XPS spectra often simplifies the presence of the different possible oxygen related species to three contributions: bulk oxides, molecular water and a mix of hydroxide species which in some cases also includes traces of contamination,[31] and carbon related species.[13]

In this report, we show the experimental detection of different oxygen related species on a STO (001) surface exposed to water vapor by AP-XPS, and we further interpret the data in terms of water molecule dissociation at the surface and photon induced water oxidation surface reactions. We further demonstrate the presence of these species in different metal oxide perovskites which easily expose TiO_2 terminated surfaces and the need to considerate them as active elements in surface screening phenomena of ferroelectric Ti based oxides.

EXPERIMENTAL METHODS:

AP- XPS experiments were performed at the NAPP endstation of the CIRCE beamline (BL-24) at the ALBA synchrotron radiation facility. The photon energy range at CIRCE is 100 eV-2000 eV. The endstation is equipped with a Phoibos 150 NAP electron energy analyzer. The analyzer is provided with four differentially pumped stages connected by small apertures. A set of electrostatic lenses focuses the electrons though the apertures to maximize transmission. Such set-up allows keeping the detector in Ultra High Vacuum while the sample is at a maximum pressure of 20 mbar.[32-33] The total electron energy resolution in the experimental conditions used for the high-resolution spectra was better than 0.3 eV. Further details about the system can be found elsewhere.[34]

Three different metal Ti-based oxide perovskite structures were studied: STO and BTO single crystals, and PZT thin films. Additionally, we also added another ferroelectric material with no Ti

sites as it is $BiFeO_3$ (BFO) thin films for comparison. STO (001) single crystals were provided by Crystec, GmbH. Commercially available substrates are mechanically polished single-crystals and their surfaces usually contain a mixture of two terminations, but commonly SrO termination is the minority, and we assume it to be below 40% of the total surface area, while the rest is TiO_2 terminated.[35] BTO (001) single crystals were acquired from SurfaceNet GmbH. $PbTi_{0.8}Zr_{0.2}O_3$ (PZT) thin film was grown on STO (001)[36] and finally, an epitaxial BFO (001) thin film on $SrRuO_3$ (SRO)-covered $DyScO_3$ (001) single-crystal substrates was prepared by pulsed laser deposition (PLD) as explained somewhere else.[37] STO sample was cleaned by heating to 300 ºC at 0.1 mbar of O_2 pressure. The evolution of the C1s peak was monitored until only a small broad peak was observed (see Figure S1). Increasing exposure time of the surface to O_2 did not originate further changes in the C1s spectra. Then the chamber was evacuated down to ~ 6.5×10^{-8} mbar and cooled down to 23ºC and water vapor was dosed into the chamber. Water was previously degassed by several freeze-pump-thaw cycles. The BTO single crystal and the other ferroelectric thin films were cleaned by heat treatment up to 300 to 400 ºC overnight in high vacuum conditions (~10^{-7} mbar). In these cases, a small amount of adventitious carbon was also observed at lower temperatures and is assumed to sit atop the surface uniformly and not influence the results. In this experiment, two different water pressures were investigated, corresponding to RH of ~5% and ~10% respectively.

High-resolution XPS spectra for the Sr3d, Ba4d, Bi4f, Pb4f, Zr3p, Ti2p, O1s and C1s core levels were obtained. Spectra acquired at the three different environmental conditions are shown in Figure 1. Spectra have been normalized in the "y" axes to the intensity of the bulk peak to take into account the loss of intensity due to electron inelastic scattering when travelling through the gas phase. Please notice that scale for C1s spectra are shown multiplied by 5. The fitting of all

XPS spectra peaks (not all shown, see some of them in Figure S2) was performed using the CasaXPS software with a combination of Gaussian/Lorentzian functions in the ratio of 70:30 after a Shirley subtraction except for the gas phase peak were a 30:70 ratio was used (see Supporting Information section B for a detailed description of the fitting methodology).

RESULTS AND DISCUSSION:

The O1s spectrum shows a complex structure of peaks as observed in Figure 2a. These peaks were assigned to different adsorbate species according to reported XPS measurements regarding water adsorption on TiO_2 terminated surfaces,[2] on perovskites,[31] and on BTO thin films.[15] The lowest binding energy (BE) peak corresponding to bulk oxide was found at 530.5 eV, similar to previously reported in the literature (Figure 2a). This BE was calibrated by taking as a reference the position of the C1s C-C adventitious carbon (energy fixed at 284.8 eV measured before annealing of the substrate in O_2 to clean it). Five additional peaks were considered to fit the O1s region, four corresponding to surface adsorbates plus a fifth peak located at +(5.5 ± 0.1) eV from the oxide peak, corresponding to the water gas phase (Figure 2a). The four oxygen-related adsorbate peaks were positioned at ΔBE = +(1.0±0.1) eV, ΔBE = + (1.8±0.1) eV, ΔBE = + (2.5±0.1) eV and ΔBE = + (3.6±0.2) eV from the bulk oxide peak. The peak closer to the oxide peak in TiO_2, STO and BTO has been consistently related to the presence of hydroxyl groups in general. For the case of TiO_2 terminated surfaces, this peak can be associated with two types of hydroxyl groups: the terminal hydroxyl group (Ti-OH) and a bridging hydroxyl group (Ox-H),[2, 11, 15, 38] which can be considered as hydroxyl groups incorporated in the lattice[15] (hereafter named "lattice OH"). For STO thought, we also have to consider the contribution of hydroxylated SrO terminated surfaces, which should contribute to this peak. The peak at ΔBE ~ 1.8 eV from the oxide has been related

to carbon oxide molecules (-COx) in studies on alcohol adsorption on STO,[13] or to carbonate species for BTO and STO surfaces exposed to CO_2.[14, 39] We corroborate this association by the combined monitoring of the O1s peak at ΔBE ~ 1.8 eV from the oxide and the C1s spectra; in the C1s spectrum taken before annealing of the STO surface, a wide peak at ΔBE ~289 eV is clearly observed corresponding to carbonates formed during exposure to atmospheric conditions. During annealing in O_2 atmosphere the O1s peak at ΔBE ~ 1.8 eV named "-CO_x" from the oxide diminishes along with the C1s peak associated to carbonate and other carbon peaks confirming its correlation with carbon related species. C1s peaks however were not totally removed in the procedure used and thus, even after annealing, a small contribution in the C1s spectra is observed (Figure 1d). Peaks located in the band between ΔBE ~ 2.4 eV and ΔBE ~3.6 eV from the oxide have been usually associated with adsorbed water on the surface.[2, 38, 40-41] However, studies of water dissociation on metals[30, 42] revealed that O1s spectra of adsorbed water could have different BE within this range depending on the nature of water, with molecules forming a water multilayer showing the highest BE in this range, while adsorbed water molecules bounded to -OH groups (that is, hydrated –OH terminations) contribute with the lowest BE.[30, 42] In addition to that, previous XPS studies also suggest the contribution in the lowest part of this BE band of chemisorbed water molecules, that is,"pseudo-dissociated" water[2,15] following an hydroxylation and protonation process (creating a pair of terminal and lattice -OH groups in a nearby position maybe also interacting through soft hydrogen bonds), followed by a back reaction to form a water molecule again with a small energy barrier of ~0.4 eV between the two states.[43] Finally, more recent studies of XPS on TiO_2 terminated surfaces extend the contribution to the lower part of this BE band to all types of chemisorbed oxygen species including those taking the form of peroxide groups.[5,44] In our case, we found that in order to fit the O1s spectra when water pressure is

increased (Figure 1a), it was necessary to consider two peaks located at the above mentioned positions (ΔBE ~ 2.5 eV and ΔBE ~ 3.6 eV from the oxide). We associate the peak at ΔBE ~ 3.6 eV from the oxide to molecularly adsorbed water bounded to other water molecules and according to the previous discussion, the peak at ΔBE ~ 2.5 eV from the oxide can have contributions from hydrating water molecules and chemisorbed oxygen species, from pseudo-dissociated water to peroxide groups (hereafter named surface oxygen peak).

Coverage of surface adsorbates containing oxygen was estimated from the intensities of the peaks used to fit the O1s region using a multilayer attenuation model,[45-46] and quantitatively analyzed following the procedure used by Newberg et al,[47,40] taking into account the theoretical inelastic mean free path (IMFP) of electrons through the different layers. Our model is similar to the one used recently to study water adsorption on perovskites[31, 48], iron oxides[49] or $LiNbO_3$[40] surfaces using AP-XPS, and renders the relative variations of peak intensity for each considered species when comparing spectra taken with two different incident energies, 700 eV and 1000eV (depth profile).[48] A visual description of this variation is shown in Figure 2b which plots a percentage variation of the species contribution with respect to an averaged value as a function of the depth of the out-coming electrons: filled bars correspond to the partial contribution of each species measured at 1000 eV and empty bars correspond to the partial contribution of the same species at 700 eV (spectra shown in Figure S4). The exact calculation of this contributions is described in the supplementary material, but the visual meaning is that a species that shows a higher empty bar means that measured electrons should be originated closer to the external surface (i.e. surface in contact with the gas) than a species showing a lower empty bar (and obviously the opposite if we check the height of the filled bars). Thus, the height of the empty bars directly correlates with a stronger superficial contribution, but considering that the differences between the

three intermediate peaks are small and might not be determining, our proposal for the distribution of the different oxide species over the sample adsorbates layer is depicted in the scheme shown in Figure 2c. Following this model we consider that the bulk oxide is covered mainly by a hydroxylated layer (terminal and lattice –OH) of thickness t_{OH}. In agreement with the data of Figure 2b, we support this idea with the fact that the main chemical environment of –OH groups should include the lattice oxygen and thus be closer to the oxide, even it can extend further along the adsorbates layer and include –OH groups that might tight to Ti or Sr ions or water molecules. In a second stage, we place a layer of both, COx species and chemisorbed surface oxygen species, with thickness t_{COx} and t_{SurfO} respectively. This layers can in fact be merged and finally all of them are mainly covered by a molecular water layer with thickness t_{H2O} (see section B3 of Supplementary Information for a detailed explanation of the model). The atomic densities of the layers were calculated from the density of the bulk counterparts. The photoionization cross-section of O1s for all species is considered to be constant. The IMFP for each layer was calculated using the NIST Standard Reference IMFP Database 71 software v1.2. with the Gries inelastic scattering model.[50]

Finally, surface oxygen vacancies can be monitored by checking the presence of shoulders in the low BE side of the Ti^{4+} $2p_{3/2}$ peak (corresponding to Ti^{4+}) due to reduced Ti species, *i.e.* Ti^{3+}. In our measurements surface oxygen vacancies are not observed in the Ti $2p_{3/2}$ peak (see Figure 1b). Nevertheless our samples were all previously exposed to atmospheric conditions so we conclude that all surface oxygen vacancies have been compensated before the experiments began. No differences in the shape of $Ti2p_{3/2}$ neither the Sr3d peaks are observed before and after water exposure (see Figure 1b, 1c).

Figure 1a shows the evolution of the O1s spectrum upon the increase of water pressure. In the inset, showing the differential spectra, it can be observed that all the peaks obtained from the decomposition of the O1s region show a dependence with the increase of water pressure. The quantification of the coverage evolution upon water pressure obtained following the model previously explained is shown in Figure 3a. It is clearly seen that the main effect of water pressure increase to the maximum water pressure is the formation of a complete monolayer of water, starting from almost no physically adsorbed water molecules. The increase in water content and adsorption has a minimal effect on the surface carbonate species that only shows minor variations all over the pressure range and also after temperature increase up to 200 ºC. Regarding the left two peaks taken into account for the spectra decomposition, corresponding to hydroxyl species and surface oxygen species, both show a progressive increase with pressure but following different trends. The surface oxide species show a stronger increase from very low values after the initial water exposure, followed by a tendency to saturation to less than half a monolayer for higher water pressures. Instead, the hydroxyls initial coverage is already considerable, of about half a monolayer, and it increases to higher values for high water coverage. This initial value is unusually high considering that after the heating treatment we applied to the surface to clean contamination, all hydroxylating groups associated to TiO_2 surfaces should be removed.[3-4] First of all, it is to mention that the absolute value as expressed in ML depends on the definition of the hydroxyls monolayer thickness as explained in the Supporting Information, which may differ among different works. Still, it is difficult to explain this high degree of hydroxylation at the initial stage after heat treatment. Several works point to the fact that SrO terminated surfaces are prone to show a higher degree of hydroxylation at room temperature,[8, 51] that could explain the initial high coverage of –OH layer, in agreement with the consideration that the percentage of SrO terminated surface can

be of up to 40%. Beyond this, we cannot dismiss that a) this peak has an extra contribution from other species b) depicts the presence of remaining hydroxylated compounds contaminating the surface after the cleaning process or c) denotes a certain degree of surface reconstruction or permanent superoxidation not able to be removed at 300 ºC that could enhance the binding of these groups to the surface. In any case, the annealing process applied for the preparation of this oxide perovskite surface is the same that can be applied to ferroelectric perovskites, thus leading to similar initial conditions to further compare experimental results.

Upon temperature increase (Figure 3b), adsorbed water molecules decrease as expected to about 0.1 ML at 200 ºC. However, even though surface oxygen peak also decreases with increasing temperature, the presence of hydroxyls on the surface is enhanced by increasing temperature. The total calculated thickness for the adsorbates layer at 2.5 mbar (corresponding to approximately an RH of 10%) is of about 1 nm (see Figure S5).

Water interaction with $SrTiO_3$ surfaces in both, SrO and TiO_2 terminations can take different paths: a) simple physical adsorption and/or formation of hydrogen bonds with the surface and among water molecules,[43] b) acid-based reactions, that is chemisorption or dissociative adsorption of the water molecules leading to hydroxylation and protonation of the surface,[8, 10, 43] and c) a wide range of redox reactions, involving oxygen transfer from the water molecules to the surface, for example interacting with surface oxygen vacancies,[2, 11, 15] or oxidative water reactions,[20-21] including those based on hole transfer from the surface.[28] The main reactions are summarized in Figure 4.

Physisorbed water is considered to be present especially for TiO_2 terminated surfaces even at very low water pressures.[8] Still, the predominant sites for water physisorption are lattice hydroxides,

i.e. protonated lattice oxides with which water tends to form hydrogen bonds, and can adopt different orientations as a function of the surface termination (SrO and TiO_2).[8] Both surface terminations can hydroxylate at different stages of water exposure as starting from completely pure surface in vacuum conditions,[51] even SrO seems to be more prone to hydroxylate easier. Besides, for very low water pressures, oxygen vacancies present at the surface are well known to promote dissociation of water which is taken as an oxidizing agent to fill up the surface oxygen vacancies and simultaneously transferring the proton to an adjacent O atom from the lattice after a surface protonation reaction, leading to the generation of a pair of lattice hydroxyl groups –OxH, contributing to the hydroxyl peak.[2, 11, 15] In our case, any possible surface oxygen vacancy has already been compensated since the $SrTiO_3$ single crystal was already previously exposed to atmospheric conditions, so the starting point is a predominantly lattice hydroxylated surface, as stated by the initial half monolayer coverage of hydroxyls groups, as observed in Figure 3a. These hydroxyl species are strongly bounded to the surface as evidenced by its trend over temperature observed in Figure 3b: at 200ºC, the coverage of the hydroxyl species is slightly enhanced as compared to room temperature, pointing out that probably they correspond to SrO hydroxylation groups,[8] since the initial surface treatment was not able to remove them as should be expected for –OH groups tight to TiO_2 terminated surfaces.[3-4]

Even in already hydroxylated surfaces, further hydroxylation of the TiO_2 terminated surfaces can happen in the form of water dissociative adsorption, by creating Ti-OH terminal hydroxyl groups plus surface protonation, and/or water pseudo-dissociation processes (followed by a back reaction to form a water molecule again). In any case, it is well known that surface hydrophilicity and wettability is strongly correlated with surface hydroxylation,[31, 40] so the increase of molecular water adsorption (H_2O peak) is expected to correlate with the presence of enough hydroxyls

coverage and a reasonable enhancement of the hydrated –OH terminations, *i.e.* water attached to –OH groups via hydrogen bonds. All of these processes contribute to the surface oxygen peak and could explain the initial enhancement of the surface oxygen peak upon water exposure from vacuum to 1 mbar together with the moderate enhancement of the hydroxyls coverage.

Considering a hydroxylated and hydrated surface as a starting point, further adsorption of water can easily happen in the form of oxidative water dissociation, especially at TiO_2 terminated surfaces, due to the known catalytic effect of Ti sites as compared to other metal sites, thought oxidation at hydroxylated SrO terminated surfaces cannot be completely neglected. Oxidative reaction processes that starts with the dissociation of water molecules at the Ti sites include first the generation of a terminal hydroxyl group Ti-OH, that can be followed by a further oxidation of the hydroxyl group to generate different types of surface peroxide species ($Ti\text{-}O^-$, Ti-O-OH, $Ti{=}O_2^-$) that should strongly contribute to what we called surface oxygen peak.[20-21] Thus, oxidative adsorption processes should be detected as the simultaneous enhancement of the two peaks; hydroxyls and surface oxyde.

STO is known to perform poorly as a water oxidation catalyst. In this sense, water oxidative processes are not expected to be predominant under atmospheric conditions, but cannot be excluded in the experimental conditions of XPS measurements. This is confirmed by the beam overexposure enhanced catalytic activity shown in Figure 5. The spectra corresponding to fresh surface spots as a function of time for a water vapor pressure of 2.5 mbar show a constant hydroxyls coverage, saturation of water molecules coverage and a slight increase of the surface oxygen peak that could be attributed to surface hydration via hydrated –OH terminations (Figure 5a and c). Instead, beam overexposure has a major impact in both, the hydroxyls and surface oxygen species peaks as shown in Figure 5 b and c. This suggests that the generation of holes by

X-ray irradiation induces the acceleration of oxidative reactions. Some DFT calculations indicate that the main active sites for hole transfer from the bulk to the surface are mediated by water molecules adsorbed on protonated bridge oxygens (lattice hydroxyls or Ox-H attached to a water molecule).[28] In this case, the catalytic reaction starts from a hydrated lattice Ox-H and by further oxidation reactions, transforms the water molecule in Ti-OH species and other peroxide species releasing protons and finally oxygen. This surface oxidation can become a cyclic process of transformation of water adsorbed molecules in oxygen and protons, also steaming into surface hydroxylation process that could still boost surface water adsorption. The enhancement of the two corresponding peaks on beam exposure is clearly seen in Figure 5b and c, for the two experiments. It has to be taken into account that beam exposure can also affect the first spectra taken, however the exposure time scales between measure and oxidation differ by one order of magnitude, being the minimal time needed to obtain the first spectra of the order of 2 minutes, while the beam exposure time scales shown in Figure 5b and c for "damage" effects is of the order of 10 to 20 minutes.

The effect of TiO_2 surface on water oxidative adsorption processes as measured by XPS should therefore not be limited to $SrTiO_3$. In this sense, different Ti perovskite surfaces were analyzed, and contrasted with similar surfaces based on other metals such as Fe. O1s spectra taken on BTO, PZT and BFO were decomposed using the same peak assignment (see detailed information on the fitting parameters for each spectra in Table S1). Figure 6 shows the results on spectra taken at 1 mbar of water vapor pressure for each material: the peaks assigned to the different oxygen related adsorbates are observed with different relative intensity depending on the material. It's important to notice that the study was done on surfaces as used for atomic force microscopy experiments: the samples were exposed to atmospheric conditions, whether the surface was reconstructed or

not, and only a vacuum annealing was performed on the as received samples. As a counterpart, this leads to a relative intensity of the COx peak that in some cases is larger than for the STO surface, but nevertheless in all of them the calculated thickness of the COx is lower than 0.5 ML, and it turns out to be strongly spot dependent.

Figure 6 clearly shows that while the surface oxygen peak in PZT and BTO shows a dominant contribution, in BFO its intensity strongly diminishes even below the hydroxyls peak and becomes almost residual. This probably denotes the presence of water molecules hydrating the surface and linked to hydroxyl groups by H-bonds. These results are in agreement with the mentioned fact that for TiO_2 terminated surfaces, there should be and enhancement of water catalytic processes mediated by the presence of Ti, that is significantly lost for the BFO surface, reinforcing the idea that this peak is mainly associated to the TiO_2 terminated surfaces, with less significant contribution from the SrO terminated surface.

Although it seems clear that the presence of Ti^{4+} can play an important role on the different oxygen species formed at the surfaces of these materials it is premature to extract conclusions from this sole data because there are other factors than can also be determinant. One of the important factors would be the polarization state of the materials. The need to screen stray electric fields generated by the ferroelectric polarization at the surface should certainly impact on the event of surface oxidative reactions and modify the type of oxygen-related species present on the surface. The different species and reactions that can take place on the surface described here (see Figure 4) involve the formation of some ionic species, such as protons and hydroxyl groups with direct impact as screening agents,[52] but also a wide range of peroxide species and subspecies of water oxidative reactions that could play a role in surface reconstruction and corrugation effects as screening mechanisms. Finally, the protons can also easily interact with water molecules at the

surface to form H_3O^- species and move along the surface through different hoping mechanisms and modifying the acidity of the hydrated surface layer.[53] On the other side, water molecules and also hydroxyl compounds are of polar nature, and the configuration of their bonding to the surface could be modulated by the ferroelectric polarization[16, 23-24] and screening mechanisms.[15, 22, 54] As a matter of fact, it is already well known that multilayer growth of dipolar water molecules is an active screening mechanism of polar surfaces due to the thermal disorder created in the dipole alignment.[17] Finally, water layers allow the diffusion of other ionic species, facilitating electrical screening as already observed experimentally on different materials such as $LiNbO_3$,[40] graphene[55] or NaCl.[56] Once the different contribution to the XPS spectra from oxygen species known to be present at STO surfaces is established, current work is under progress for a better understanding of the role of those species on the screening mechanisms on ferroelectric Ti based perovskites.

CONCLUSIONS:

In summary, the dissociation of water and associated oxidative processes at coarse metal oxide perovskite surfaces, i.e., exposed to ambient, have been investigated by ambient AP-XPS under different water vapor pressures. We have detected the presence of four different oxygen related species in the O1s spectra besides the expected peak corresponding to bulk oxygen, that have been assigned to hydroxyl groups, either bound to Ti^{4+} and Sr^{2+} metal sites or lattice oxygen, hydrated water molecules either physisorbed or pseudo-dissociated, light contribution of carbonates due to inherent contamination of atmospheric exposed surfaces and finally and more remarkably, complex peroxide compounds resulting from surface oxidative reactions. We propose a model for the composition of the adsorbates layer that should prevail for environmental conditions, for which the hydroxyl groups remain on top of the oxide surface, overlaid by the carbonate and peroxide species at a higher level, and overall covered by physisorbed water molecules. We have described

different surface redox reactions for metal oxide perovskites leading to the observed surface oxygen related species, and we have determined the environmental conditions for which each of them is favored. Particularly, surface water oxidation cycle is enhanced by X-ray beam irradiation, leading to a higher coverage of peroxide species after beam overexposure. Peroxide species resulting from surface oxidative reactions on surfaces exposed to water are correlated with the presence of Ti^{4+} ions, which are observed to expressly promote surface oxidation and water dissociation as compared to other metals: in this sense, the enhanced water catalytic action of Ti^{4+} ions should be taken into account when studying screening effects in Ti-based ferroelectric perovskites.

ASSOCIATED CONTENT

Supporting Information:

Section A: Figure S1: XPS spectra of C1s and O1s regions for $SrTiO_3$ single crystals under cleaning process by annealing in O_2 pressure at high temperatures. Section B: Detailed description of the fitting methodology for O1s region and attenuation model. Figure S2: Decomposition of XPS spectra of O1s regions for STO at all pressures (shown in Figure 1a, with results plotted in Figure 3a) and T (results plotted in Figure 3b). Table S1: Fitting parameters used for decomposition of O1s region in Figure 6. Table S2: Parameters used in the multilayer electron attenuation model. Figure S3: Comparison of coverage calculations for different parameters used. Section C: Figure S4: O1s spectra measured at 700 eV and 1000 eV on the same spot at residual water vapour gas conditions (pressure < 10-3 mbar) after the pressure and temperature experiments. Figure S5: Evolution of calculated thickness of the adsorbates layer as a function of the water pressure. Figure

S6: Survey spectra of the three different ferroelectric perovskites mentioned in the manuscript measured at 700 eV.

ACKNOWLEDGMENT

Authors would like to acknowledge Prof. P.Paruch of Université de Genève, who kindly provided PZT thin film samples and Prof. B. Noheda for kindly providing BFO thin films. Financial support was obtained under projects from the Spanish Ministerio de Economía y Competitividad (MINECO) under projects FIS2015-73932-JIN and MAT2016-77852-C2-1-R (AEI/FEDER, UE). ICN2 acknowledges support from the Severo Ochoa Program (MINECO, Grant No. SEV-2013-0295), and ICMAB acknowledges support from the Severo Ochoa Program (MINECO, Grant No. SEV-2015-0496). This work was partially funded by 2017-SGR-579 and 2017-SGR-668 projects from the Generalitat de Catalunya. The authors would like to thank the support of ALBA staff for the successful performance of the measurements at CIRCE beamline from the ALBA Synchrotron Light Source.

REFERENCES

1. Björneholm, O.; Hansen, M. H.; Hodgson, A.; Liu, L.-M.; Limmer, D. T.; Michaelides, A.; Pedevilla, P.; Rossmeisl, J.; Shen, H.; Tocci, G.; Tyrode, E.; Walz, M.-M.; Werner, J.; Bluhm, H., Water at Interfaces. *Chemical Reviews* **2016,** *116* (13), 7698-7726.
2. Ketteler, G.; Yamamoto, S.; Bluhm, H.; Andersson, K.; Starr, D. E.; Ogletree, D. F.; Ogasawara, H.; Nilsson, A.; Salmeron, M., The Nature of Water Nucleation Sites on TiO2(110) Surfaces Revealed by Ambient Pressure X-ray Photoelectron Spectroscopy. *The Journal of Physical Chemistry C* **2007,** *111* (23), 8278-8282.
3. Walle, L. E.; Borg, A.; Uvdal, P.; Sandell, A., Experimental evidence for mixed dissociative and molecular adsorption of water on a rutile ${\text{TiO}}_{2}(110)$ surface without oxygen vacancies. *Physical Review B* **2009,** *80* (23), 235436.
4. Walle, L. E.; Borg, A.; Johansson, E. M. J.; Plogmaker, S.; Rensmo, H.; Uvdal, P.; Sandell, A., Mixed Dissociative and Molecular Water Adsorption on Anatase TiO2(101). *The Journal of Physical Chemistry C* **2011,** *115* (19), 9545-9550.
5. Krivtsov, I.; Ilkaeva, M.; Salas-Colera, E.; Amghouz, Z.; García, J. R.; Díaz, E.; Ordóñez, S.; Villar-Rodil, S., Consequences of Nitrogen Doping and Oxygen Enrichment on Titanium Local Order and Photocatalytic Performance of TiO2 Anatase. *The Journal of Physical Chemistry C* **2017,** *121* (12), 6770-6780.
6. Wang, L.-Q.; Ferris, K. F.; Herman, G. S., Interactions of H2O with SrTiO3(100) surfaces. *Journal of Vacuum Science & Technology A: Vacuum, Surfaces, and Films* **2002,** *20* (1), 239-244.
7. Evarestov, R. A.; Bandura, A. V.; Alexandrov, V. E., Adsorption of water on (001) surface of SrTiO3 and SrZrO3 cubic perovskites: Hybrid HF-DFT LCAO calculations. *Surface Science* **2007,** *601* (8), 1844-1856.
8. Guhl, H.; Miller, W.; Reuter, K., Water adsorption and dissociation on SrTiO3 revisited: A density functional theory study. *Physical Review B* **2010,** *81* (15), 155455.
9. Hinojosa, B. B.; Van Cleve, T.; Asthagiri, A., A first-principles study of H2O adsorption and dissociation on the SrTiO3(100) surface. *Molecular Simulation* **2010,** *36* (7-8), 604-617.
10. Voigts, F.; Argirusis, C.; Maus-Friedrichs, W., The interaction of H2O with Fe-doped SrTiO3(100) surfaces. *Surface and Interface Analysis* **2011,** *43* (6), 984-992.
11. Li, W.; Liu, S.; Wang, S.; Guo, Q.; Guo, J., The Roles of Reduced Ti Cations and Oxygen Vacancies in Water Adsorption and Dissociation on SrTiO3(110). *The Journal of Physical Chemistry C* **2014,** *118* (5), 2469-2474.
12. Holmström, E.; Spijker, P.; Foster, A. S., The interface of SrTiO3 and H2O from density functional theory molecular dynamics. *Proceedings of the Royal Society A: Mathematical, Physical and Engineering Science* **2016,** *472* (2193), 20160293.
13. Zhang, Y. F.; Savara, A.; Mullins, D. R., Ambient-Pressure XPS Studies of Reactions of Alcohols on SrTiO3(100). *J Phys Chem C* **2017,** *121* (42), 23436-23445.
14. Baniecki, J. D.; Ishii, M.; Kurihara, K.; Yamanaka, K.; Yano, T.; Shinozaki, K.; Imada, T.; Kobayashi, Y., Chemisorption of water and carbon dioxide on nanostructured BaTiO3–SrTiO3(001) surfaces. *Journal of Applied Physics* **2009,** *106* (5), 054109.
15. Wang, J. L.; Gaillard, F.; Pancotti, A.; Gautier, B.; Niu, G.; Vilquin, B.; Pillard, V.; Rodrigues, G. L. M. P.; Barrett, N., Chemistry and Atomic Distortion at the Surface of an Epitaxial BaTiO3 Thin Film after Dissociative Adsorption of Water. *The Journal of Physical Chemistry C* **2012,** *116* (41), 21802-21809.

16. Li, X.; Wang, B.; Zhang, T.-Y.; Su, Y., Water Adsorption and Dissociation on BaTiO3 Single-Crystal Surfaces. *The Journal of Physical Chemistry C* **2014,** *118* (29), 15910-15918.
17. Segura, J. J.; Domingo, N.; Fraxedas, J.; Verdaguer, A., Surface screening of written ferroelectric domains in ambient conditions. *Journal of Applied Physics* **2013,** *113* (18), 187213.
18. Nassreddine, S.; Morfin, F.; Niu, G.; Vilquin, B.; Gaillard, F.; Piccolo, L., Application of a sensitive catalytic reactor to the study of CO oxidation over SrTiO3(100) and BaTiO3/SrTiO3(100) ferroelectric surfaces. *Surface and Interface Analysis* **2014,** *46* (10-11), 721-725.
19. Wang, Z.; Hao, X.; Gerhold, S.; Novotny, Z.; Franchini, C.; McDermott, E.; Schulte, K.; Schmid, M.; Diebold, U., Water Adsorption at the Tetrahedral Titania Surface Layer of SrTiO3(110)-(4 × 1). *The Journal of Physical Chemistry C* **2013,** *117* (49), 26060-26069.
20. Martirez, J. M. P.; Kim, S.; Morales, E. H.; Diroll, B. T.; Cargnello, M.; Gordon, T. R.; Murray, C. B.; Bonnell, D. A.; Rappe, A. M., Synergistic Oxygen Evolving Activity of a TiO2-Rich Reconstructed SrTiO3(001) Surface. *Journal of the American Chemical Society* **2015,** *137* (8), 2939-2947.
21. Koocher, N. Z.; Martirez, J. M. P.; Rappe, A. M., Theoretical Model of Oxidative Adsorption of Water on a Highly Reduced Reconstructed Oxide Surface. *The Journal of Physical Chemistry Letters* **2014,** *5* (19), 3408-3414.
22. Shin, J.; Nascimento, V. B.; Geneste, G.; Rundgren, J.; Plummer, E. W.; Dkhil, B.; Kalinin, S. V.; Baddorf, A. P., Atomistic Screening Mechanism of Ferroelectric Surfaces: An In Situ Study of the Polar Phase in Ultrathin BaTiO3 Films Exposed to H2O. *Nano Letters* **2009,** *9* (11), 3720-3725.
23. Geneste, G.; Dkhil, B., Adsorption and dissociation of H2O on in-plane-polarized BaTiO3 (001) surfaces and their relation to ferroelectricity. *Physical Review B* **2009,** *79* (23), 235420.
24. Spanier, J. E.; Kolpak, A. M.; Urban, J. J.; Grinberg, I.; Ouyang, L.; Yun, W. S.; Rappe, A. M.; Park, H., Ferroelectric Phase Transition in Individual Single-Crystalline BaTiO3 Nanowires. *Nano Letters* **2006,** *6* (4), 735-739.
25. Krug, I.; Barrett, N.; Petraru, A.; Locatelli, A.; Mentes, T. O.; Niño, M. A.; Rahmanizadeh, K.; Bihlmayer, G.; Schneider, C. M., Extrinsic screening of ferroelectric domains in Pb(Zr0.48Ti0.52)O3. *Applied Physics Letters* **2010,** *97* (22), 222903.
26. Lampimäki, M.; Schreiber, S.; Zelenay, V.; Křepelová, A.; Birrer, M.; Axnanda, S.; Mao, B.; Liu, Z.; Bluhm, H.; Ammann, M., Exploring the Environmental Photochemistry on the TiO2(110) Surface in Situ by Near Ambient Pressure X-ray Photoelectron Spectroscopy. *The Journal of Physical Chemistry C* **2015,** *119* (13), 7076-7085.
27. Chen, H.; Nanayakkara, C. E.; Grassian, V. H., Titanium Dioxide Photocatalysis in Atmospheric Chemistry. *Chemical Reviews* **2012,** *112* (11), 5919-5948.
28. Liu, F.; Feng, N.; Wang, Q.; Xu, J.; Qi, G.; Wang, C.; Deng, F., Transfer Channel of Photoinduced Holes on a TiO2 Surface As Revealed by Solid-State Nuclear Magnetic Resonance and Electron Spin Resonance Spectroscopy. *Journal of the American Chemical Society* **2017,** *139* (29), 10020-10028.
29. Migani, A.; Blancafort, L., What Controls Photocatalytic Water Oxidation on Rutile TiO2(110) under Ultra-High-Vacuum Conditions? *Journal of the American Chemical Society* **2017,** *139* (34), 11845-11856.
30. Zeng, Z. H.; Greeley, J., Characterization of oxygenated species at water/Pt(111) interfaces from DFT energetics and XPS simulations. *Nano Energy* **2016,** *29*, 369-377.

31. Stoerzinger, K. A.; Hong, W. T.; Azimi, G.; Giordano, L.; Lee, Y.-L.; Crumlin, E. J.; Biegalski, M. D.; Bluhm, H.; Varanasi, K. K.; Shao-Horn, Y., Reactivity of Perovskites with Water: Role of Hydroxylation in Wetting and Implications for Oxygen Electrocatalysis. *The Journal of Physical Chemistry C* **2015,** *119* (32), 18504-18512.
32. Bluhm, H., Photoelectron spectroscopy of surfaces under humid conditions. *J Electron Spectrosc* **2010,** *177* (2-3), 71-84.
33. Starr, D. E.; Liu, Z.; Havecker, M.; Knop-Gericke, A.; Bluhm, H., Investigation of solid/vapor interfaces using ambient pressure X-ray photoelectron spectroscopy. *Chem Soc Rev* **2013,** *42* (13), 5833-5857.
34. Perez-Dieste, V.; Aballe, L.; Ferrer, S.; Nicolas, J.; Escudero, C.; Milan, A.; Pellegrin, E., Near Ambient Pressure XPS at ALBA. *J Phys Conf Ser* **2013,** *425*, 072023.
35. Sanchez, F.; Ocal, C.; Fontcuberta, J., Tailored surfaces of perovskite oxide substrates for conducted growth of thin films. *Chem Soc Rev* **2014,** *43* (7), 2272-2285.
36. Gariglio, S.; Stucki, N.; Triscone, J.-M.; Triscone, G., Strain relaxation and critical temperature in epitaxial ferroelectric Pb(Zr0.20Ti0.80)O3 thin films. *Applied Physics Letters* **2007,** *90* (20), 202905.
37. Domingo, N.; Farokhipoor, S.; Santiso, J.; Noheda, B.; Catalan, G., Domain wall magnetoresistance in BiFeO 3 thin films measured by scanning probe microscopy. *Journal of Physics: Condensed Matter* **2017,** *29* (33), 334003.
38. Jackman, M. J.; Thomas, A. G.; Muryn, C., Photoelectron Spectroscopy Study of Stoichiometric and Reduced Anatase TiO2(101) Surfaces: The Effect of Subsurface Defects on Water Adsorption at Near-Ambient Pressures. *The Journal of Physical Chemistry C* **2015,** *119* (24), 13682-13690.
39. Song, A. Q.; Skibinski, E. S.; DeBenedetti, W. J. I.; Ortoll-Bloch, A. G.; Hines, M. A., Nanoscale Solvation Leads to Spontaneous Formation of a Bicarbonate Monolayer on Rutile (110) under Ambient Conditions: Implications for CO2 Photoreduction. *J Phys Chem C* **2016,** *120* (17), 9326-9333.
40. Cordero-Edwards, K.; Rodriguez, L.; Calo, A.; Esplandiu, M. J.; Perez-Dieste, V.; Escudero, C.; Domingo, N.; Verdaguer, A., Water Affinity and Surface Charging at the z-Cut and y-Cut LiNbO3 Surfaces: An Ambient Pressure X-ray Photoelectron Spectroscopy Study. *J Phys Chem C* **2016,** *120* (42), 24048-24055.
41. Verdaguer, A.; Weis, C.; Oncins, G.; Ketteler, G.; Bluhm, H.; Salmeron, M., Growth and structure of water on SiO2 films on Si investigated by Kelvin probe microscopy and in situ x-ray spectroscopies. *Langmuir* **2007,** *23* (19), 9699-9703.
42. Casalongue, H. S.; Kaya, S.; Viswanathan, V.; Miller, D. J.; Friebel, D.; Hansen, H. A.; Nørskov, J. K.; Nilsson, A.; Ogasawara, H., Direct observation of the oxygenated species during oxygen reduction on a platinum fuel cell cathode. *Nature Communications* **2013,** *4*, 2817.
43. Wendt, S.; Matthiesen, J.; Schaub, R.; Vestergaard, E. K.; Lægsgaard, E.; Besenbacher, F.; Hammer, B., Formation and Splitting of Paired Hydroxyl Groups on Reduced TiO2(110)

Physical Review Letters **2006,** *96* (6), 066107.
44. Gao, Y.; Masuda, Y.; Koumoto, K., Light-Excited Superhydrophilicity of Amorphous TiO2 Thin Films Deposited in an Aqueous Peroxotitanate Solution. *Langmuir* **2004,** *20* (8), 3188-3194.
45. Kurbatov, G.; Darqueceretti, E.; Aucouturier, M., Characterization of Hydroxylated Oxide Film on Iron Surfaces and Its Acid-Base Properties Using Xps. *Surface and Interface Analysis* **1992,** *18* (12), 811-820.

46. McCafferty, E.; Wightman, J. P., Determination of the concentration of surface hydroxyl groups on metal oxide films by a quantitative XPS method. *Surface and Interface Analysis* **1998,** *26* (8), 549-564.
47. Newberg, J. T.; Starr, D. E.; Yamamoto, S.; Kaya, S.; Kendelewicz, T.; Mysak, E. R.; Porsgaard, S.; Salmeron, M. B.; Brown, G. E.; Nilsson, A.; Bluhm, H., Formation of hydroxyl and water layers on MgO films studied with ambient pressure XPS. *Surface Science* **2011,** *605* (1), 89-94.
48. Stoerzinger, K. A.; Hong, W. T.; Crumlin, E. J.; Bluhm, H.; Biegalski, M. D.; Shao-Horn, Y., Water Reactivity on the LaCoO3 (001) Surface: An Ambient Pressure X-ray Photoelectron Spectroscopy Study. *J Phys Chem C* **2014,** *118* (34), 19733-19741.
49. Yamamoto, S.; Kendelewicz, T.; Newberg, J. T.; Ketteler, G.; Starr, D. E.; Mysak, E. R.; Andersson, K. J.; Ogasawara, H.; Bluhm, H.; Salmeron, M.; Brown, G. E.; Nilsson, A., Water Adsorption on alpha-Fe2O3(0001) at near Ambient Conditions. *J Phys Chem C* **2010,** *114* (5), 2256-2266.
50. J., P. C.; A., J.; F., S., NIST databases with electron elastic-scattering cross sections, inelastic mean free paths, and effective attenuation lengths. *Surface and Interface Analysis* **2005,** *37* (11), 1068-1071.
51. Iwahori, K.; Watanabe, S.; Kawai, M.; Kobayashi, K.; Yamada, H.; Matsushige, K., Effect of water adsorption on microscopic friction force on SrTiO3(001). *Journal of Applied Physics* **2003,** *93* (6), 3223-3227.
52. Lee, H.; Kim, T. H.; Patzner, J. J.; Lu, H.; Lee, J.-W.; Zhou, H.; Chang, W.; Mahanthappa, M. K.; Tsymbal, E. Y.; Gruverman, A.; Eom, C.-B., Imprint Control of BaTiO3 Thin Films via Chemically Induced Surface Polarization Pinning. *Nano Letters* **2016,** *16* (4), 2400-2406.
53. Adhikari, S.; Garcia-Castro, A. C.; Romero, A. H.; Lee, H.; Lee, J.-W.; Ryu, S.; Eom, C.-B.; Cen, C., Charge Transfer to LaAlO3/SrTiO3 Interfaces Controlled by Surface Water Adsorption and Proton Hopping. *Advanced Functional Materials* **2016,** *26* (30), 5453-5459.
54. Pancotti, A.; Wang, J.; Chen, P.; Tortech, L.; Teodorescu, C.-M.; Frantzeskakis, E.; Barrett, N., X-ray photoelectron diffraction study of relaxation and rumpling of ferroelectric domains in BaTiO3 (001). *Physical Review B* **2013,** *87* (18), 184116.
55. Verdaguer, A.; Cardellach, M.; Segura, J. J.; Sacha, G. M.; Moser, J.; Zdrojek, M.; Bachtold, A.; Fraxedas, J., Charging and discharging of graphene in ambient conditions studied with scanning probe microscopy. *Applied Physics Letters* **2009,** *94* (23), 233105.
56. Verdaguer, A.; Segura, J. J.; Fraxedas, J.; Bluhm, H.; Salmeron, M., Correlation between Charge State of Insulating NaCl Surfaces and Ionic Mobility Induced by Water Adsorption: A Combined Ambient Pressure X-ray Photoelectron Spectroscopy and Scanning Force Microscopy Study. *The Journal of Physical Chemistry C* **2008,** *112* (43), 16898-16901.

TOC:

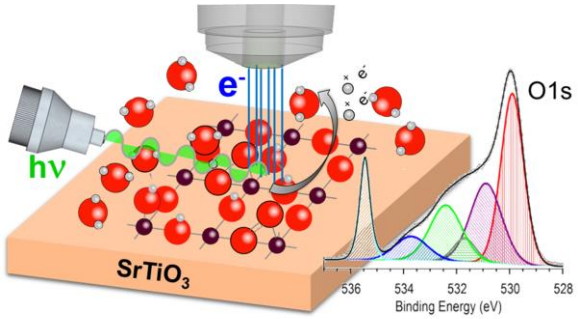

FIGURE CAPTIONS:

Figure 1. XPS spectra of STO single crystal (001) surface in three different ambient conditions at 700 eV: high vacuum of 10^{-7} mbar (black line), 1 mbar of H_2O pressure (light blue line) and 2.5 mbar of H_2O pressure (dark blue line). a) O1s region of XPS spectra. The inset shows the differential spectra upon water presence after subtraction of the 10^{-7} mbar spectra. b) Ti2p region c) Sr3d region and d) C1s region of XPS spectra under the different RH.

Figure 2. a) Decomposition of the O1s XPS spectra at 700 eV of incident X-ray energy of STO single crystal (001) surface at 1 mbar of water pressure into the 6 the different contributions from right to left: bulk oxide (red peak filled with vertical lines), hydroxyl groups (purple peak with decreasing diagonal lines), carbonate species (grey peak with horizontal lines), surface oxygen species including peroxides (green peak with decreasing diagonal lines) and water molecules (dark blue peak with increasing diagonal lines) (see further explanation in the text). The final peak on the left hand side corresponds to the water in gas phase (light blue peak with increasing diagonal lines) b) Depth profile considering XPS spectra acquired at different incident energies. c) Schematic of the multilayer electron attenuation model used to determine coverages with the distribution of the considered species over the adsorbate layer thickness.

Figure 3 Coverage of the different components of the O1s spectra at 700 eV in terms of monolayers as calculated from the model: a) as a function of water pressure and b) at 1 mbar and at two different temperatures: RT (filled bars) and 200 ºC (patterned bars)

Figure 4 Schematic drawing of the different types of water interactions with the surface. a) pseudo-dissociative water adsorption b) molecular water physisorption c) redox reaction on oxygen vacancies and d) schematic sequences of subspecies appearing in surface oxidative water adsorption and catalytic reactions.

Figure 5. Differential XPS spectra taken at 2.5 mbar and 700 eV under different conditions. a) Evolution over time at t_1 = 3500 s and t_2 = 5400 s on different spots and b) evolution after different number of XPS spectra acquisitions on the same spot, denoting the effect of beam exposure on the water oxidation dynamics. c) Composed picture of the coverage levels of the different species on a homogeneous scaled time bar for all the measurements. Filled symbols (blue ● for H_2O, purple ◒ for hydroxyls, green ◓ for the surface oxygen peak, and grey ⊗ for the carbonate species) correspond to the effect of time of exposure at 1 mbar of water pressure with t_1 and t_2 of the order of minutes, and measurements done at different spots. Empty square and triangle symbols for each curve correspond to the effect of beam overexposure imposed to time, that is, the acquisition of various spectra (#1, #2 and up to #3 different shots) at the same spot.

Figure 6. Decomposition of XPS spectra of O1s regions at 700 eV for a) PZT thin films b) BTO single crystals and c) BFO thin films. The legend of the peaks corresponds to the distribution of the peaks from right to left as follows: bulk oxide, hydroxils, carbonate species, surface oxygen including peroxide species, adsorbed molecular water and gas phase water. The color code is the same as in Figure 2.

Figure 1

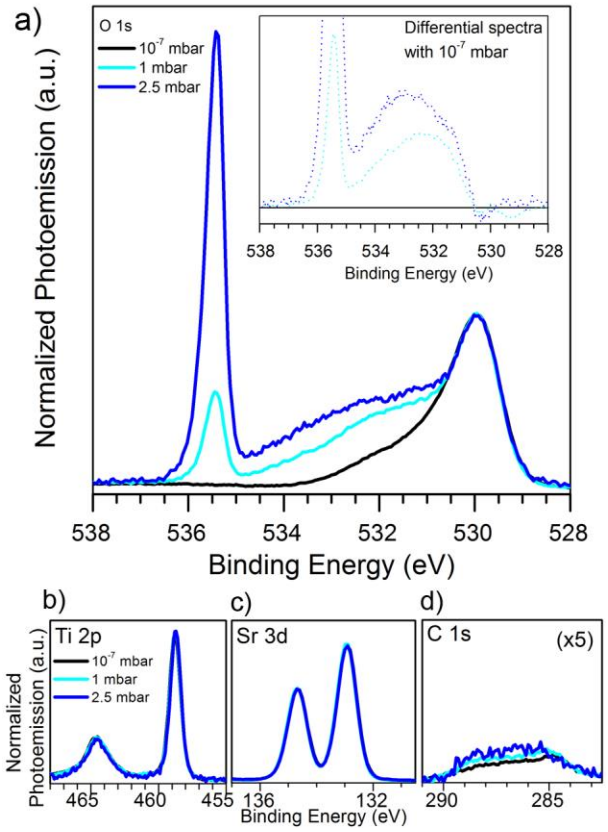
a)
O 1s
10^-7 mbar
1 mbar
2.5 mbar
Differential spectra
with 10^-7 mbar
538 536 534 532 530 528
Binding Energy (eV)
Normalized Photoemission (a.u.)
538 536 534 532 530 528
Binding Energy (eV)
b)
Ti 2p
10^-7 mbar
1 mbar
2.5 mbar
c)
Sr 3d
d)
C 1s
(x5)
Normalized Photoemission (a.u.)
465 460 455
136 132
290 285
Binding Energy (eV)

Figure 2

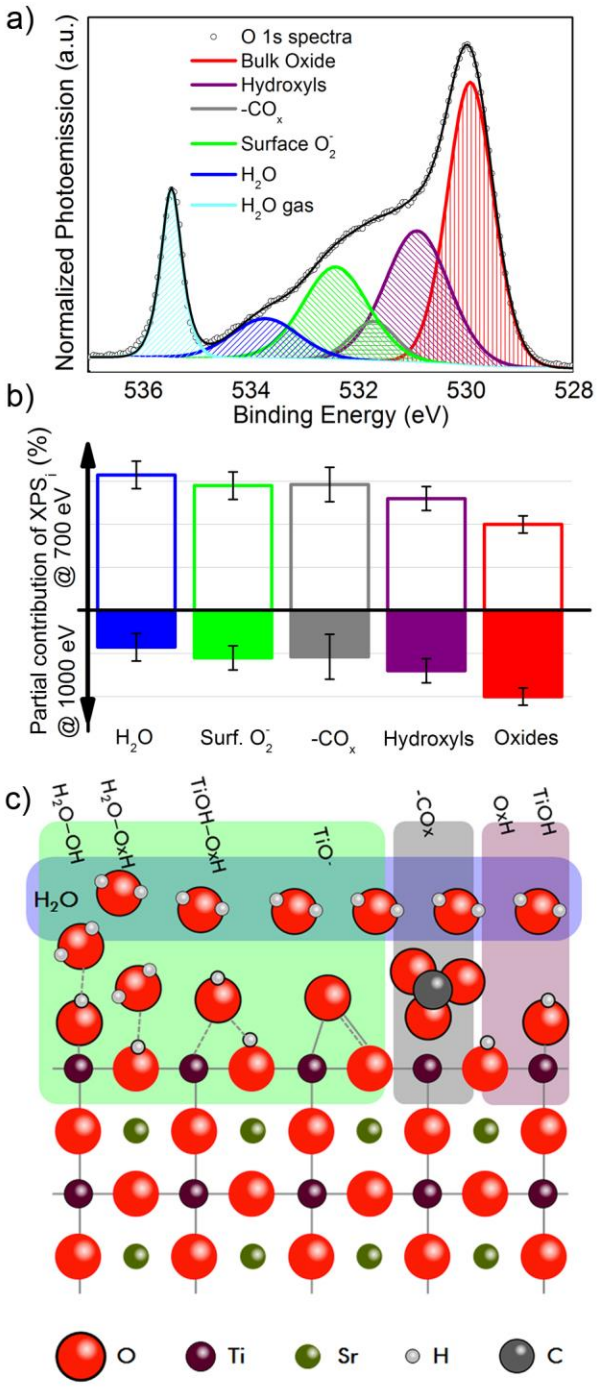
a)
O 1s spectra
Bulk Oxide
Hydroxyls
-CO$_x$
Surface O$_2^-$
H$_2$O
H$_2$O gas
Normalized Photoemission (a.u.)
536
534
532
530
528
Binding Energy (eV)
b)
Partial contribution of XPS$_i$ (%)
@ 700 eV
@ 1000 eV
H$_2$O
Surf. O$_2^-$
-CO$_x$
Hydroxyls
Oxides
c)
H$_2$O–OxH
TiOH–OxH
Ti:O$^-$
-COx
OxH
TiOH
H$_2$O
O
Ti
Sr
H
C

Figure 3

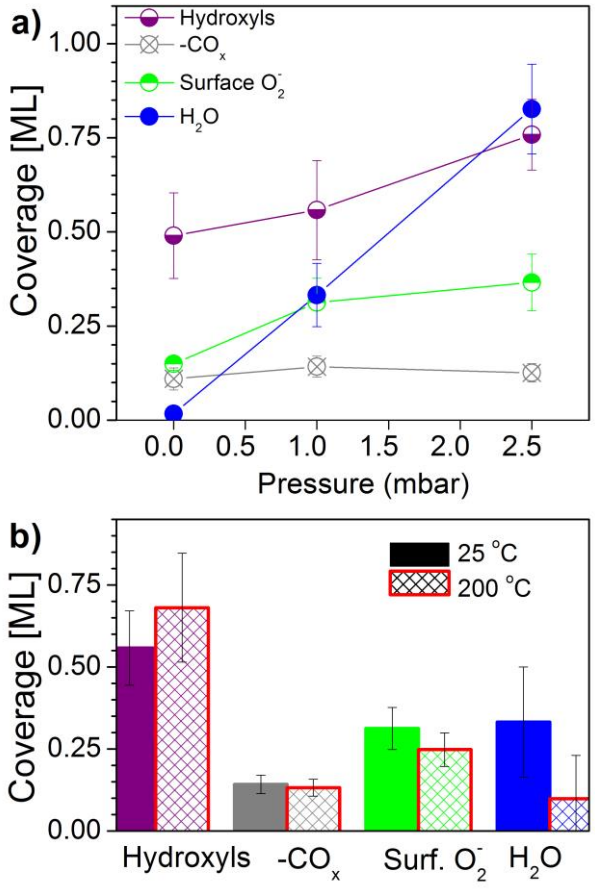
a)
Hydroxyls
-CO$_x$
Surface O$_2^-$
H$_2$O
Coverage [ML]
1.00
0.75
0.50
0.25
0.00
0.0
0.5
1.0
1.5
2.0
2.5
Pressure (mbar)
b)
25 °C
200 °C
Coverage [ML]
0.75
0.50
0.25
0.00
Hydroxyls
-CO$_x$
Surf. O$_2^-$
H$_2$O

Figure 4

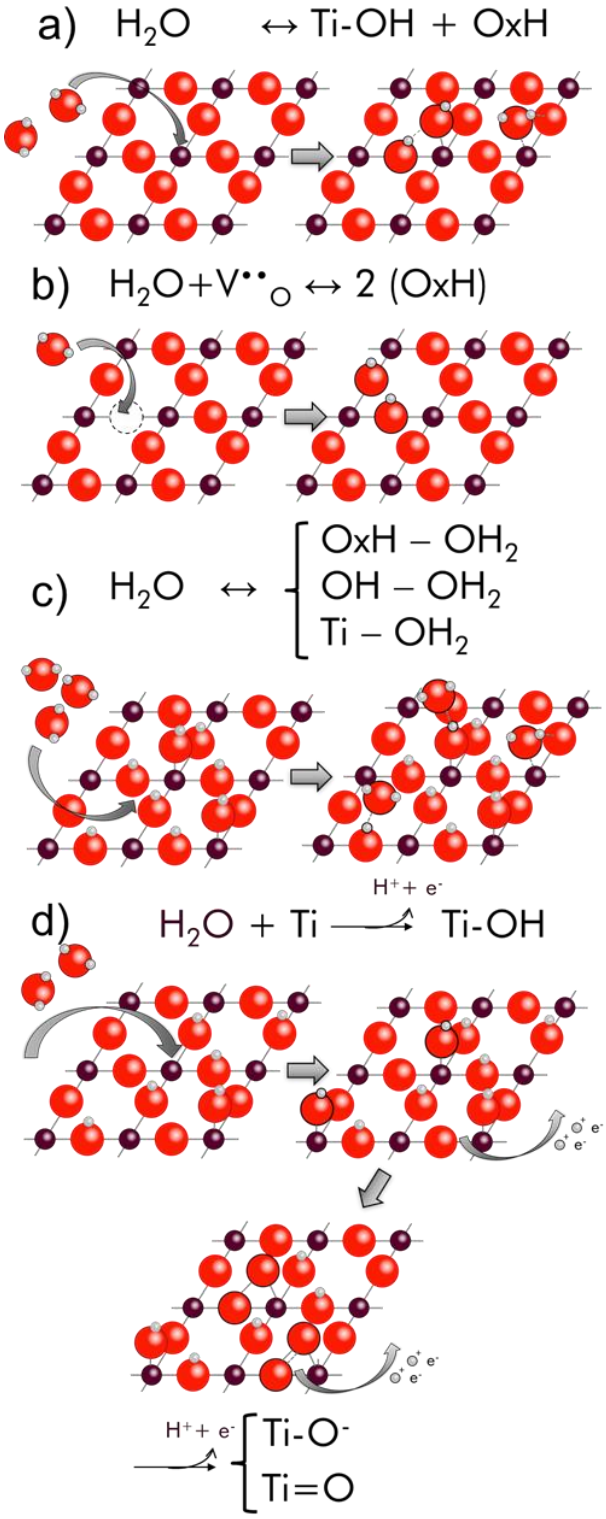
a) H_2O ↔ Ti-OH + OxH
b) $H_2O+V^{\bullet\bullet}_O$ ↔ 2 (OxH)
c) H_2O ↔ $OxH - OH_2$ / $OH - OH_2$ / $Ti - OH_2$
d) H_2O + Ti → Ti-OH
$H^+ + e^-$
$H^+ + e^-$ → Ti-O⁻ / Ti=O

Figure 5

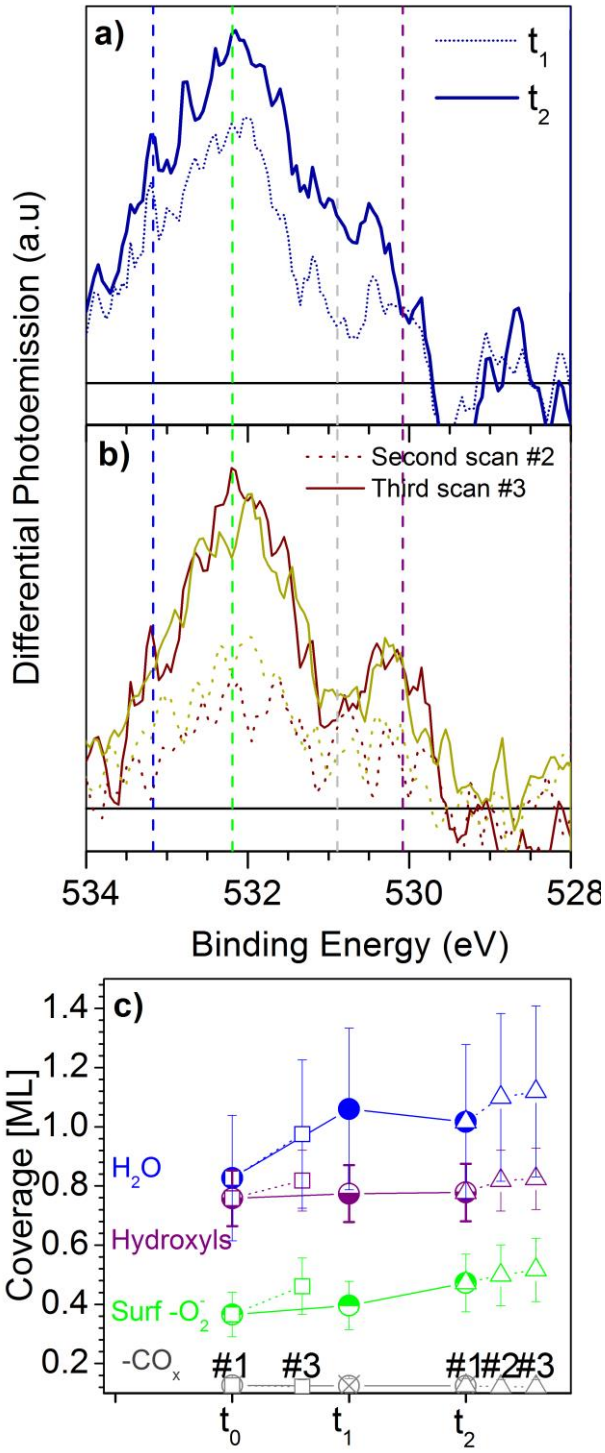
a)
t1
t2
b)
Second scan #2
Third scan #3
Differential Photoemission (a.u)
534
532
530
528
Binding Energy (eV)
c)
Coverage [ML]
1.4
1.2
1.0
0.8
0.6
0.4
0.2
H2O
Hydroxyls
Surf -O2-
-COx
#1
#3
#1#2#3
t0
t1
t2

Figure 6

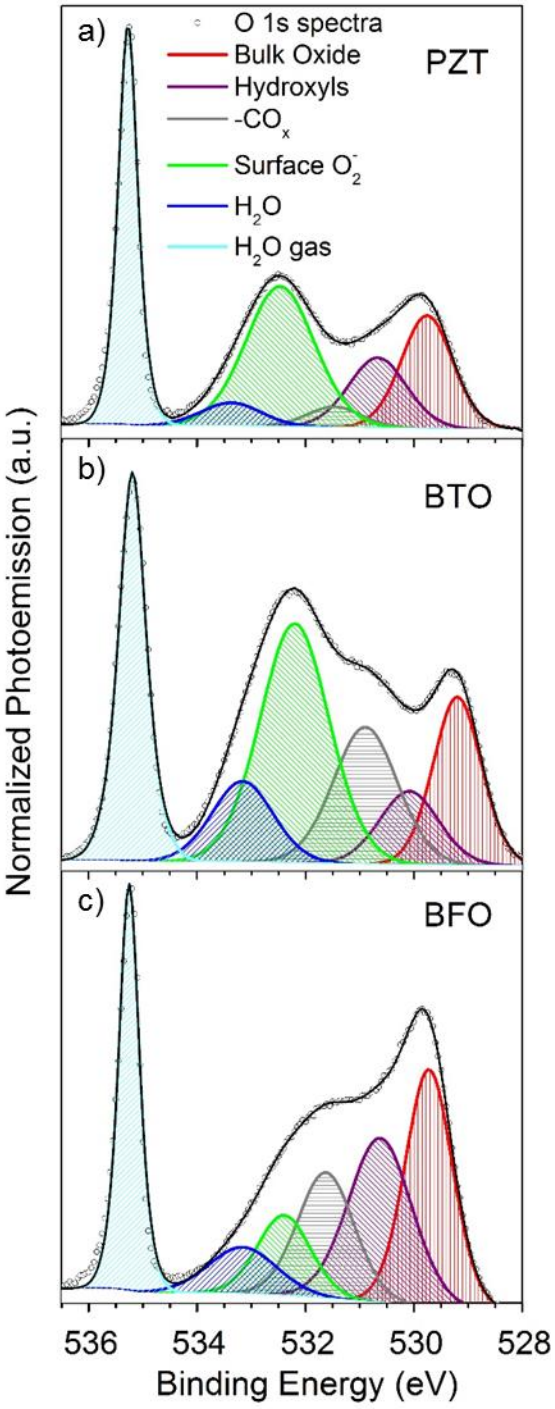
a)
O 1s spectra
Bulk Oxide
Hydroxyls
-CO$_x$
Surface O$_2^-$
H$_2$O
H$_2$O gas
PZT
b)
BTO
c)
BFO
Normalized Photoemission (a.u.)
536
534
532
530
528
Binding Energy (eV)